Research Article Vol. 2, No. 1 / January 2015 / Optica 40

Miniature multioctave light source based on a monolithic microcavity

Wei Liang,[1] Anatoliy A. Savchenkov,[1] Zhenda Xie,[2] James F. McMillan,[2] Jan Burkhart,[2] Vladimir S. Ilchenko,[1] Chee Wei Wong,[2] Andrey B. Matsko,[1,*] and Lute Maleki[1]

[1]OEwaves Inc., 465N. Halstead Str., Pasadena, California 91107, USA

[2]Optical Nanostructures Laboratory, Center for Integrated Science and Engineering, Solid-State Science and Engineering, and Mechanical Engineering, Columbia University, New York, New York 10027, USA

*Corresponding author: andrey.matsko@oewaves.com

Received 27 August 2014; revised 12 November 2014; accepted 13 November 2014 (Doc. ID 221896); published 15 January 2015

Optical microresonators are ideal tools for the reduction of the threshold of optical parametric oscillation based on four-wave mixing. Usually, the efficiency and bandwidth of the resonant process are interdependent due to stringent phase matching requirements leading to limitation of the bandwidth of the spectrum generated for a given pump power. We demonstrate a continuous-wave low-threshold resonant optical parametric oscillator with optical spectral span ranging from 0.36 to 1.6 μm. Harmonic generation is observed when a MgF_2 microresonator characterized by quality factor approaching 10^{10} is pumped either at 780 nm, with a standard distributed-feedback semiconductor laser, or at 698 nm, with a reflective amplifier. Pump power does not exceed 25 mW. The nonlinear process is phase matched due to $\chi^{(3)}$-facilitated interaction of different mode families of the resonator. The optical harmonics generated can be used to seed high-power visible lasers, generate correlated photon pairs, and perform spectroscopy measurements.

OCIS codes: (190.4380) Nonlinear optics, four-wave mixing; (190.4970) Parametric oscillators and amplifiers; (230.4910) Oscillators.

http://dx.doi.org/10.1364/OPTICA.2.000040

1. INTRODUCTION

Continuous-wave (cw) power-efficient parametric generation of coherent and spectrally pure optical signals at an arbitrary optical wavelength is challenging because of phase mismatch among the interacting electromagnetic waves [1,2]. The most commonly used approaches including birefringent [3,4], noncollinear [5,6], and quasi-phase matching techniques [7–10] are bandwidth-limited. Broadband frequency conversion techniques based on coherent Raman scattering [11–16], plasmonics [17–19], as well as metamaterials and hollow-core photonic crystal fibers [20–24] frequently require high intensity levels of the optical pump to be efficient, and are unsuitable for cw applications. Optical microresonators lend a solution to these problems. Optical parametric oscillators (OPOs) and optical parametric frequency converters based on monolithic microresonators with quadratic [25–30] and cubic [31–43] nonlinearities are not subject to the above restriction. Microresonators are suitable for tunable OPOs [44–47]. Additionally, microresonator-based devices pave the way for realizing chip-scale nonlinear and quantum optics experiments.

Whispering-gallery-mode resonators (WGMRs) [48,49] are among the most suitable structures for the excitation of nonlinear optics processes with low light level. In particular, resonators made with CaF_2 and MgF_2 are excellent candidates for the observation of broadband nonlinear optical phenomena, since these materials are highly transparent in the wavelength range of 150 nm–10 μm [50]. The finesse of these resonators can be very large, and the highest demonstrated finesse in optics ($F > 10^7$) has been achieved with a CaF_2 resonator [51]. Therefore, even small pump power levels reach the threshold of the nonlinear processes associated with the nonlinearity of these materials. Furthermore, the spectral properties of WGMRs are well understood and there exist multiple efficient techniques for coupling light in and out of these structures.

Basically, it is possible to fabricate a resonator to achieve phase matching among any set of resonant optical waves involved in a nonlinear optical interaction.

There are four basic nonlinear processes observed in WGMRs. Resonant optomechanical oscillation (OMO) and resonant stimulated Brillouin scattering (SBS) have the lowest comparable power thresholds [52]. Optical parametric oscillation (OPO) based on the four-wave mixing (FWM) process has a higher threshold [31–41,43], while stimulated Raman scattering (SRS) [53] has the highest threshold. OMO and SBS can be suppressed efficiently by the selection of proper resonator geometry that does not support the phase matching of the given processes. SRS frequently competes with OPO since it has much weaker phase matching requirements and can involve high-order WGMs that have higher Q-factors. By choosing the geometry of the resonator properly and by introducing optimal coupling, it is possible to make OPO operation favorable over the other nonlinear processes.

The generation of broad optical spectra is one of the challenges related to microresonator-based OPOs. Octave-spanning optical combs have been demonstrated, but with hundreds of milliwatts of power coupled to microresonators [54,55]. Here, the power of the frequency sidebands was rather small because of reduced pump coupling efficiency, as well as the distribution of the pump power among multiple frequency sidebands. To generate high-power harmonics, the number of sidebands has to be reduced preferably to only a pair, so that the first-order hyperparametric oscillation would dominate frequency comb generation. An efficient way for extending the sidebands over an octave or a larger span has to be found to make the output of the oscillator useful. A severe constraint generally exists between the efficiency and bandwidth of the FWM process, resulting from the stringent requirement for phase matching of this nonlinear resonant process [40].

Here we report on a study of a strongly nondegenerate OPO using a high-Q crystalline magnesium fluoride (MgF_2) WGMR. The resonator host material features a small thermorefractive constant, excellent mechanical stability, hardness, and optical transparency, confirmed by the production of very-high-Q WGMRs [56–59]. Both hyperparametric oscillation and Kerr frequency comb generation were observed in the MgF_2 resonators operating in the anomalous group velocity dispersion (GVD) regime [59,60]. In this study, we use this material to realize a strongly nondegenerate OPO operating in the nominally normal GVD regime.

While hyperparametric oscillations have been observed previously in the normal GVD regime, the resultant spectra were much narrower than the spectra reported in this work. The reason is in the physical principle underlying the nonlinear phenomena. Dark soliton mode locking can exist in normal GVD nonlinear resonators [61–70]; however, the frequency spectrum of the pulses generated is rather narrow. The mode crossing phenomenon can be utilized to modify the local GVD in a resonator to achieve mode locking [71–74]; however, this phenomenon also produces relatively narrow frequency spectra compared with the spectral width reported in this paper.

We demonstrate the efficient generation of spectral harmonics separated by hundreds of terahertz, and covering more than two octaves, from a single optical pump [75]. The study reported here complements the very recent observation of tunable cw multicolor emission in the visible from fused silica microspherical WGMRs, based on third-harmonic generation and Raman-assisted third-order sum-frequency generation [76–78]. In the case reported here oscillator phase matching is achieved since the FWM process involves several mode families of the resonator, similarly to [78]. No linear interaction among resonator modes (mode crossing) is required to achieve phase matching in this configuration. We argue that spectral engineering of the resonator enables the generation of a desirable optical spectrum within a very broad wavelength range, limited primarily by the transparency of the resonator host material. This conclusion is supported by the very recent observation of frequency harmonics separated by 18 THz from the pump frequency, generated in a morphology-engineered microcavity [79]. Because of the significant frequency difference between the OPO harmonics, it is possible to separate them efficiently using a diffraction grating. This feature is important for the generation of quantum correlated photon pairs from the resonator. The OPO signal can also be used to seed high-power visible lasers, and for molecular spectroscopy.

We observed three distinct regimes of oscillation: (i) generation of equidistant spectral harmonics separated from each other by 50 THz in a single OPO process; (ii) generation of multiple harmonics originating from two independent OPO processes; and (iii) generation of multiple harmonics covering the entire visible range and spanning from UV to near-IR. The harmonic generation was observed at two different wavelengths, 780 and 698 nm. A self-injection-locked distributed-feedback (DFB) semiconductor laser was used in the first experiment. This technique of pumping was validated previously [80–83]. A reflective semiconductor optical amplifier was utilized in the second experiment to pump a resonator mode with bandwidth eight orders of magnitude less than the gain bandwidth of the amplifier. This technique is novel and promising, as the system demonstrated resembles a new type of an external cavity laser. It was used in this experiment since a 698 nm semiconductor laser was not readily available to us.

The paper is organized as follows: in Section 2, we describe our experiments. A theoretical explanation of the oscillation observed is presented in Section 3. Section 4 concludes the paper.

2. DESCRIPTION OF EXPERIMENT

We built an enclosure for the WGMR to make it contamination-free for use outside the clean room environment (Fig. 1). The enclosure is environmentally stable and is capable of preserving a 100 nm air gap between the resonator and the coupling prism surface. The temperature of the package was stabilized to a millikelvin level.

The resonator was fabricated from a MgF_2 preform by mechanical polishing, and had a 7 mm diameter, with a thickness of 100 μm [9.9 GHz free spectral range (FSR)]. We used an evanescent prism coupler to send and retrieve the pump light to/from the resonator, and the loaded quality factor exceeded 5×10^9 at 780 nm and reached 10^{10} at 698 nm.

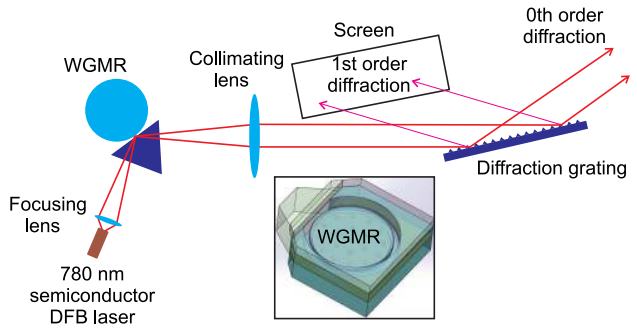

Fig. 1. Schematic diagram of the experimental setup. The inset shows a drawing of the packaged MgF_2 resonator used in the experiments. The 7 mm diameter resonator was inserted into an enclosure. The enclosure was used for the protection of the open resonator from dust particles as well as for stabilizing the air gap between the surface of the resonator and the coupling prism.

The resonator was pumped with either a 780 nm DFB semiconductor laser (with about 1 MHz linewidth, when free running) or with a 698 nm semiconductor optical amplifier chip with10 nm gain bandwidth and 5 mW output power. The DFB laser was self-injection locked [80–83] to a selected resonator mode, while the reflective amplifier started to lase when coupled to the resonator mode. We used two different pump wavelengths to demonstrate that the process does not depend significantly on the pump wavelength. Two different pump sources were utilized to show the flexibility of the configuration.

A. Oscillation Resulting from 780 nm Pumping

In the first experiment, a high-power 780 nm Eagleyard DFB laser was used to pump the resonator. A GRIN lens was utilized to focus the laser emission to the mode of the resonator. The lasing threshold with respect to the laser current was measured to be 33 mA. The free-running linewidth of the laser exceeded 1 MHz, so the self-injection locking [80–83] technique was used to narrow the linewidth of the laser and also to pump the resonator. By sweeping the current of the DFB laser, different modes of the resonator were interrogated, and when the gap between the resonator surface and the prism coupler was adjusted to be compatible at 780 nm, we observed the parametric process generating visible light. The linear contrast of the WGM spectrum was typically 30% with this optimal loading and the modal match between the laser and the WGMs. We observed visible parametric lines with laser current as low as 43 mA (≈1 mW optical power pumped into the resonator) due to the high Q of the resonator modes.

At the output of the prism coupler, the light was collimated and sent to a holographic reflective grating (1800 lines per millimeter) to separate the lights of different colors generated (Fig. 1). The first-order diffracted beam was projected on a paper screen for observation, and a digital camera was used to record the visible parametric lines when sweeping the laser across selected modes. The collimated beam was also coupled into an optical fiber using a fiber launcher. The collected light was sent to an optical spectrum analyzer (OSA) for recording the spectra of the emitted radiation.

We observed that some of the lines were not generated simultaneously when the laser was tuned across a particular mode. A particular combination of visible lines was generated when the laser was injection locked at a particular detuning from the center of the mode. If the detuning was changed, the combination of generated harmonics also changed, providing a tunable means for generating different lines. This observation is somewhat similar to the observation of change of mode-locked regimes in the case of Kerr frequency comb generation [84,85].

The oscillation started with less than 1 mW of optical power coupled into the mode. By pumping the resonator with 20 mW of cw light at 780 nm, we observed the generation of anti-Stokes harmonics at 620 and 684 nm (at approximately 50 and 100 THz from the carrier) as well as corresponding Stokes harmonics [Fig. 2(a)]. The power of the harmonics exceeded 10 μW, which is a rather large value for OPO harmonics detuned so far from the pump light.

A slight increase in the optical pump power or a change in the detuning between the pump frequency and the corresponding resonator mode resulted in the generation of a denser spectrum [Fig. 2(b)], with new frequency harmonics produced. We found that all the harmonics originated from a pair of best phase-matched OPO processes at 52.4 and 74.5 THz, as well as from SRS.

By increasing the power of the pump light further, we observed harmonic generation spanning the spectrum from UV (360 nm) to near-IR (1500 nm). A controllable change in the temperature of the resonator and/or the pump wavelength tuned the oscillation frequency and switched the wavelengths generated.

The spectrum of the signal of the OPO driven far above its threshold is shown in Fig. 3. It is aperiodic and is produced by mixing the harmonics generated initially (Fig. 2). Interestingly, the densest spectrum is generated at the blue side of the

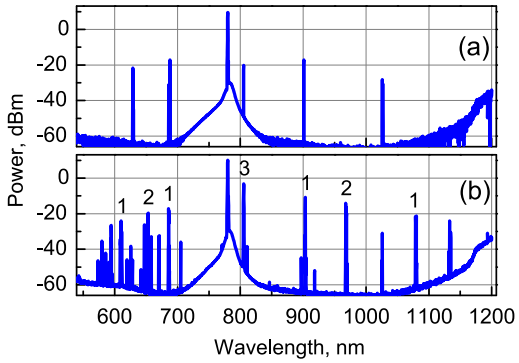

Fig. 2. (a) Demonstration of OPO including two pairs of frequency sidebands only. The resonator is pumped with 20 mW of 780 nm light. The intensity nonuniformity of the harmonic sidebands arises from the wavelength-dependent coupling efficiency. (b) Optical spectrum of the light leaving the resonator when pumped with 25 mW of optical power. The optical harmonics generated in the resonator result from a pair of OPO processes (52.4 THz, line 1, and 74.5 THz, line 2, from the carrier). The Stokes sideband generated in the vicinity of the carrier (12.3 THz away to the red side, line 3) results from the SRS process. All visible lines of the spectrum can be explained by FWM of the harmonics generated in the processes 1, 2, and 3.

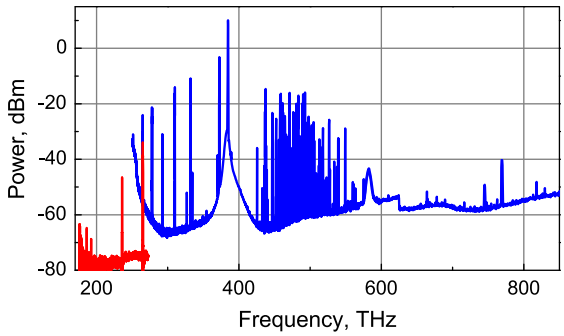

Fig. 3. Frequency spectrum of the oscillation signal for the case where optical pumping exceeds the threshold by approximately two orders of magnitude (50 mW of pumping). The spectrum is taken using two different OSAs. The closest line to the carrier on the red side is the first-order SRS Stokes line. The spectrum covers more than two octaves.

optical pumping. This is the region of normal GVD of the undisturbed resonator modes. On the other hand, the density of the WGMs and their Q increase toward the blue side, since the loading of the resonator decreases with decreasing wavelength. That is why the probability of optimal conditions for the FWM process increases on the blue side of the generated spectra.

The coherence of the OPO harmonics was not verified experimentally. It can be predicted, though, that it is comparable to the coherence of the pump light. The behavior of the oscillator is similar to the behavior of the Kerr frequency comb oscillators. The phase matching depends strongly on the frequency detuning of the pumping laser as well as on the frequency of the resonator. The generation of optical harmonics occurs in different mode families, as required by phase matching conditions. Since all those features are specific for the resonant parametric oscillation, we can expect that the light generated is highly coherent; we plan to verify the coherence in future investigations.

To show that the OPO is phase matched due to the interaction of different mode families of the resonator (see, e.g., [78]), we mapped the far-field distribution of the harmonics exiting the resonator. The resonator output was sent to a reflective diffraction grating and the grating output was displayed on a screen. A picture of the light observed is shown in Fig. 4, which illustrates the realization of three different OPO regimes. To the far left of the plot, one can see ellipses corresponding to the pump far-field profile leaving the resonator. The brightness of the spot is low because the pump wavelength is barely visible with our camera. The harmonics generated are located at the center as well as on the right-hand side of the plot. The beam profiles of the OPO harmonics frequently have two lobes, implying that higher order modes are involved in the process.

Our WGMR had a dense spectrum of high-Q optical modes and the OPO operation was sensitive to the detuning of the pump laser frequency from the corresponding mode. The performance also depended on the power and wavelength of the pump. The spatial alignment of the laser beam was critically important for the selection of a particular mode of interest. We had to carefully stabilize all degrees of freedom

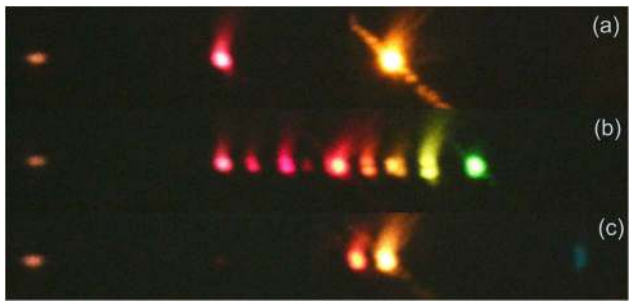

Fig. 4. Light emitted by the WGMR pumped with 780 nm light observed on a screen placed after a diffraction grating. (a)–(c) are obtained by injection locking the laser to different modes of the resonator at different pump powers, and different resonator temperatures. The spot due to the pump light is to the far left of each plot. The spot is elongated along the horizontal direction due to the elliptical shape of the laser beam itself. The spots on the right, corresponding to the harmonics generated, can be single or (more frequently, but not always) have two lobes. Colors from red to blue are visible.

to achieve stable operation of the OPO. The self-injection locking ensured that the laser frequency followed the WGM frequency within a several gigahertz dynamic range (it corresponds to more than 2 K resonator temperature change). Independent change of the temperature of the laser chip as well as the laser current allowed modifying the frequency detuning within the locking range, which approximately corresponded to the half width at half-maximum of the corresponding WGM. Alignment stability was achieved by the reduction of the optical path length. As a result, the operation of the setup was stable and controllable in the laboratory environment.

B. Oscillation Resulting from 698 nm Pumping

We performed a similar experiment by pumping the resonator with 698 nm light and observed very similar results as compared to those described above. The difference was that a semiconductor optical amplifier chip was used to pump a resonator mode with 20 kHz bandwidth. Coupling was achieved due to the self-injection locking phenomenon, which resulted in the realization of a narrow-line external cavity laser, where the WGMR played the role of the external cavity.

The schematic of the device is illustrated in Fig. 5. We sent a collimated amplified spontaneous emission signal from a semiconductor optical amplifier (SOA) to a diffraction grating and then coupled the 0th diffraction order signal to the WGMR. The system started lasing when relative resonant feedback from the WGMR surpassed several percent. Emission of visible frequency harmonics can be seen clearly when the lasing power exceeds a certain threshold.

Linewidth test of the laser is performed by beating the pump light escaping the resonator with a cavity-stabilized diode laser. The accuracy of the measurement was limited by 25 kHz, which is approximately equal to the bandwidth of the pumped WGM. A more careful study has to be performed to reveal the coherence properties of the laser. The results of the study will be published elsewhere.

We were able to generate a number of wavelengths spanning from UV to near-IR for nearly the same pump power

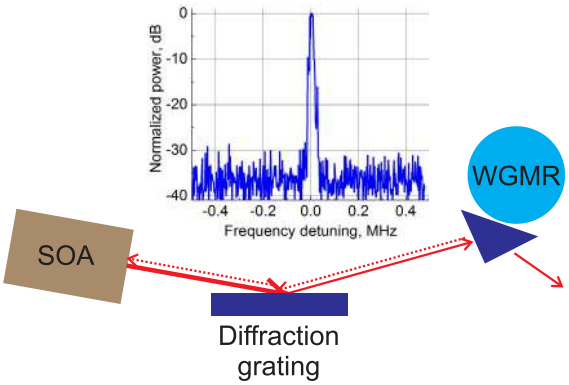

Fig. 5. Schematic of the setup of the OPO involving a reflective amplifier. The inset shows the RF signal produced by the 698 nm laser mixed with an optical local oscillator on a fast photodiode. The linewidth measured is limited by the accuracy of the measurement and is less than 25 kHz.

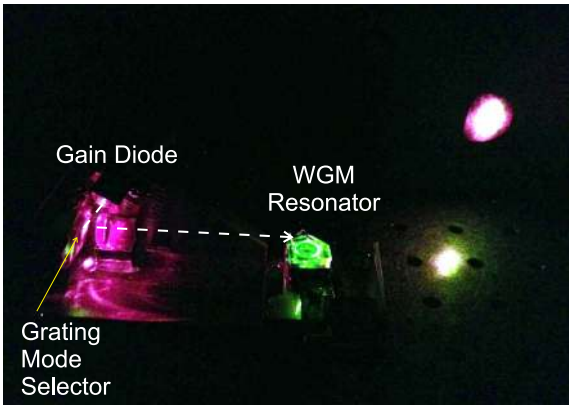

Fig. 7. Demonstration of parametric frequency conversion in the resonator pumped with 698 nm light. The pump laser, located to the left side of the picture, is glowing red, whereas the pumped resonator glows green.

as was used at 780 nm. An example of the spectrum emitted is shown in Fig. 6. The visible spectrum is captured with a CCD spectrometer (Thorlabs CCS200) and the IR is taken with an OSA. The CCD measurement is almost instantaneous, which results in a high noise floor, whereas the OSA permits long integration of the signal, revealing more spectral lines. The blue harmonics were observed visually.

Figure 7 illustrates the emission of the frequency harmonics in the setup. The resonator is pumped with red light and a bright green light emission is seen clearly. Comparing Figs. 3 and 7, one can see that the generation of the broad optical spectrum does not depend significantly on the pumping wavelength. Emission was observed in the case of pumping the resonator at both 698 and 780 nm. We expect that it will be observed at any pump wavelength located within the normal GVD wavelength region of the nonlinear resonator.

3. EXPLANATION OF PHASE MATCHING INVOLVING DIFFERENT ORDER MODES

The MgF_2 resonator has a large normal GVD at both 780 and 698 nm, which results in significant spacing asymmetry among resonator modes. The asymmetry cannot be compensated by the cross-phase modulation resulting from the nonlinearity of the material, since the nonlinear effect only adds to the mode inequidistance due to the normal GVD. Therefore, it is not expected that hyperparametric oscillation will take place in the resonator.

Let us consider a simplified case of the parametric generation of two optical sidebands with frequencies $\nu_{\pm}$ separated far from the pump frequency ν_0 [Fig. 2(a)]. To characterize the degree of mode separation, we evaluated the second-order dispersion parameter $D = 2\nu_0 - \nu_+ - \nu_-$ for the resonator (Fig. 8). The frequency of the resonator modes can be found numerically from the solution of Eq. (1) [86]:

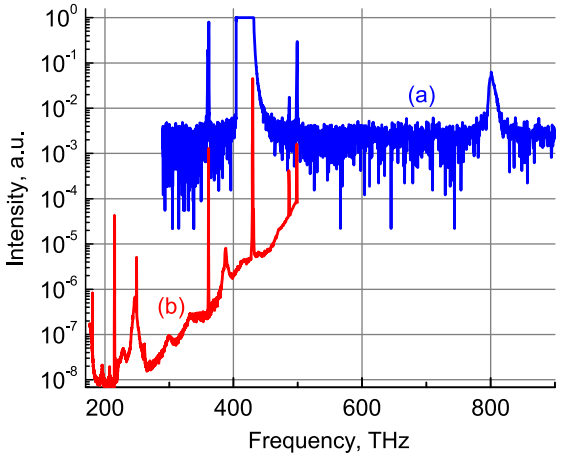

Fig. 6. Emission spectra of the resonator pumped at 698 nm taken with (a) a CCD spectrometer and (b) an OSA.

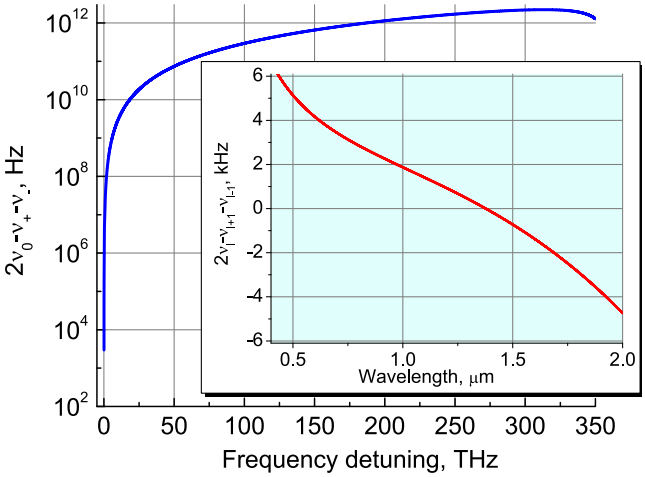

Fig. 8. Frequency difference among resonator mode triplets as a function of sideband–carrier frequency separation. The triplets involve an optically pumped mode characterized by frequency ν_0 corresponding to a wavelength of 780 nm (azimuthal index $l_0 = 36,340$) and sideband modes, characterized by frequencies ν_+ and ν_- (azimuthal indices $l_0 + \Delta l$ and $l_0 - \Delta l$, respectively). The frequency separation between the sideband and the carrier modes is determined by Δl. Inset: GVD parameter $2\nu_l - \nu_{l+1} - \nu_{l-1}$ versus pump wavelength.

$$\nu_{l,q} \simeq \frac{c}{2\pi n_0(\nu_{l,q})R}\left[l + \alpha_q\left(\frac{l}{2}\right)^{1/3} - \sqrt{\frac{n_0(\nu_{l,q})^2}{n_0(\nu_{l,q})^2 - 1}}\right], \quad (1)$$

where l is the azimuthal mode number, α_q is the qth root of the Airy function $Ai(-z)$ (q is a natural number), R is the radius of the resonator, and $n_0(\nu_{l,q})$ is the frequency-dependent refractive index of the resonator host material, which can be found using the corresponding Sellmeier equation for MgF_2. For the sake of clarity, we selected $q = 1$, evaluated the equation for different values of l, and found the corresponding lth mode frequency, ν_l. Equation (1) describes well the modes of a cylinder or sphere and is a good approximation for the fundamental mode family of a spheroid.

The dispersion parameter evaluated for the frequency harmonics supposedly generated in the fundamental mode family at 50 THz from the carrier, as shown in Fig. 2(a) (≈73 GHz, Fig. 7), is many orders of magnitude larger than the mode bandwidth of, approximately, 100 kHz. This implies that the fundamental mode family, corresponding to $q = 1$, cannot host the parametric process. Additionally, linear mode crossing [71–74] cannot compensate for the difference either, since linear interaction between the modes does not shift the position of the modes by hundreds of gigahertz.

We explain the observed OPO process to be the interaction between the fundamental mode family and the high-order vertical modes of the spheroidal resonator. Two nearly equidistant mode sequences characterized by the free spectral ranges $FSR_l = c/(2\pi n_0 R)$ and $FSR_p = FSR_l(R - r)/r$ exist in a spheroidal resonator. Here, p is the vertical number of the modes and $r < R$ is the shorter semi-axis of the spheroid [87,88]. The oscillation process involves the pumped fundamental mode with indices l and $p = 0$ and sideband modes with indices $l \pm \Delta l$ and $p \neq 0$. Using the dispersion relation derived in [87] for these modes, we can find

$$2\nu_0(l, q, p = 0) - \nu_+(l + \Delta l, q, p) - \nu_-(l - \Delta l, q, p) \simeq D - \frac{c}{2\pi n_0(\nu_{l,q})R}\frac{2(R - r)}{r}p, \quad (2)$$

where parameter D can be found from Eq. (1). Equation (2) shows that the large positive value of D is compensated if high-order vertical modes are included. The parameter D can even change its sign, moving the system from the normal to the anomalous dispersion regime. Additionally, it is known that the FWM overlap integral of the modes considered is significant [89]. Therefore, the oscillation process is favorable for the particular mode configuration. This conclusion is supported by the observation of two-lobe emission in Fig. 4, which is associated with the emission from the vertical modes [89].

The vertical mode number p does not need to be large for the generation of the observed OPO process. Our resonator has $R = 3.5$ mm and $r = 1.29$ mm, so the vertical mode family with $p = 2$ is large enough to accommodate the oscillation sidebands separated from the carrier by ≈50 THz. The selection of a proper mode pair allows reducing the dispersion parameter D by two orders of magnitude, practically for any pumped mode. Further tuning of the parameter D may require careful tuning of the pump frequency to find the proper l and p in a resonator with a fixed shape. Alternatively, the geometry of the resonator can be adjusted to create a desirable spectrum for a fixed frequency of the pump laser.

4. CONCLUSION

In conclusion, we have demonstrated experimentally and explained theoretically the generation of multioctave optical spectra produced by the OPO process with a continuously pumped WGMR. This approach has the potential for the realization of power-efficient chip-scale optical parametric oscillators operating at a wide range of frequencies in the spectral range from UV to IR. The oscillators are important for the generation of quantum correlated photon pairs directly from a continuously pumped resonator. The optical harmonics generated can also be used to seed high-power visible lasers, and for molecular spectroscopy.

FUNDING INFORMATION

Air Force Office of Scientific Research (AFOSR) (FA9550-12-C-0068); Defense Advanced Research Projects Agency (DARPA) (W911QX-12-C-0067).

REFERENCES

1. Y. R. Shen, *The Principles of Nonlinear Optics* (Wiley-Interscience, 1984).
2. R. Boyd, *Nonlinear Optics* (Academic, 2008).
3. J. A. Giordmaine, "Mixing of light beams in crystals," Phys. Rev. Lett. **8**, 19–20 (1962).
4. P. D. Maker, R. W. Terhune, M. Nisenoff, and C. M. Savage, "Effects of dispersion and focusing on the production of optical harmonics," Phys. Rev. Lett. **8**, 21–22 (1962).
5. J. Falk and J. Murray, "Efficient noncollinear single-cavity parametric oscillator," IEEE J. Quantum Electron. **5**, 356–357 (1969).
6. T. R. Zhang, H. R. Choo, and M. C. Downer, "Phase and group velocity matching for second harmonic generation of femtosecond pulses," Appl. Opt. **29**, 3927–3933 (1990).
7. J. A. Armstrong, N. Bloembergen, J. Ducuing, and P. S. Pershan, "Interactions between light waves in a nonlinear dielectric," Phys. Rev. **127**, 1918–1939 (1962).
8. N. Bloembergen and A. J. Sieveres, "Nonlinear optical properties of periodic laminar structures," Appl. Phys. Lett. **17**, 483–486 (1970).
9. C. L. Tang and P. P. Bey, "Phase matching in second-harmonic generation using artificial periodic structures," IEEE J. Quantum Electron. **9**, 9–17 (1973).
10. M. M. Fejer, G. A. Magel, D. H. Jundt, and R. L. Byer, "Quasi-phase-matched second harmonic generation: tuning and tolerances," IEEE J. Quantum Electron. **28**, 2631–2654 (1992).
11. S. E. Harris and A. V. Sokolov, "Broadband spectral generation with refractive index control," Phys. Rev. A **55**, R4019–R4022 (1997).
12. H. Kawano, Y. Hirakawa, and T. Imasaka, "Generation of high-order rotational lines in hydrogen by four-wave Raman mixing in the femtosecond regime," IEEE J. Quantum Electron. **34**, 260–268 (1998).
13. A. V. Sokolov, D. R. Walker, D. D. Yavuz, G. Y. Yin, and S. E. Harris, "Raman generation by phased and antiphased molecular states," Phys. Rev. Lett. **85**, 562–565 (2000).
14. P. M. Paul, E. S. Toma, P. Breger, G. Mullot, F. Auge, Ph. Balcou, H. G. Muller, and P. Agostini, "Observation of a train of attosecond pulses from high harmonic generation," Science **292**, 1689–1692 (2001).

15. D. D. Yavuz, D. R. Walker, M. Y. Shverdin, G. Y. Yin, and S. E. Harris, "Quasi-periodic Raman technique for ultrashort pulse generation," Phys. Rev. Lett. **91**, 233602 (2003).
16. I. P. Christov, M. M. Murnane, and H. C. Kapteyn, "High-harmonic generation of attosecond pulses in the "single-cycle" regime," Phys. Rev. Lett. **78**, 1251–1254 (1997).
17. H. J. Simon, D. E. Mitchell, and J. G. Watson, "Optical second-harmonic generation with surface plasmons in silver films," Phys. Rev. Lett. **33**, 1531–1534 (1974).
18. D. Von der Linde and K. Rzazewski, "High-order optical harmonic generation from solid surfaces," Appl. Phys. B **63**, 499–506 (1996).
19. S. Kim, J. Jin, Y.-J. Kim, I.-Y. Park, Y. Kim, and S.-W. Kim, "High-harmonic generation by resonant plasmon field enhancement," Nature **453**, 757–760 (2008).
20. G. D'Aguanno, N. Mattiucci, M. Scalora, and M. J. Bloemer, "Second-harmonic generation at angular incidence in a negative-positive index photonic band-gap structure," Phys. Rev. E **74**, 026608 (2006).
21. F. Couny, F. Benabid, P. J. Roberts, P. S. Light, and M. G. Raymer, "Generation and photonic guidance of multi-octave optical-frequency combs," Science **318**, 1118–1121 (2007).
22. H. Suchowski, K. O'Brien, Z. J. Wong, A. Salandrino, X. Yin, and X. Zhang, "Phase mismatch-free nonlinear propagation in optical zero-index materials," Science **342**, 1223–1226 (2013).
23. D. de Ceglia, S. Campione, M. A. Vincenti, F. Capolino, and M. Scalora, "Low-damping epsilon-near-zero slabs: nonlinear and nonlocal optical properties," Phys. Rev. B **87**, 155140 (2013).
24. N. Mattiucci, M. J. Bloemer, and G. D'Aguanno, "Phase-matched second harmonic generation at the Dirac point of a 2-D photonic crystal," Opt. Express **22**, 6381–6390 (2014).
25. J. U. Furst, D. V. Strekalov, D. Elser, M. Lassen, U. L. Andersen, Ch. Marquardt, and G. Leuchs, "Naturally phase-matched second-harmonic generation in a whispering-gallery-mode resonator," Phys. Rev. Lett **104**, 153901 (2010).
26. J. U. Furst, D. V. Strekalov, D. Elser, A. Aiello, U. L. Andersen, Ch. Marquardt, and G. Leuchs, "Quantum light from a whispering-gallery-mode disk resonator," Phys. Rev. Lett. **106**, 113901 (2011).
27. S. Schiller and R. L. Byer, "Quadruply resonant optical parametric oscillation in a monolithic total-internal-reflection resonator," J. Opt. Soc. Am. B **10**, 1696–1707 (1993).
28. K. Fiedler, S. Schiller, R. Paschotta, P. Kürz, and J. Mlynek, "Highly efficient frequency doubling with a doubly resonant monolithic total-internal-reflection ring resonator," Opt. Lett. **18**, 1786–1788 (1993).
29. R. Paschotta, P. Kurz, R. Henking, S. Schiller, and J. Mlynek, "82% Efficient continuous-wave frequency doubling of 1.06 μm with a monolithic MgO:$LiNbO_3$ resonator," Opt. Lett. **19**, 1325–1327 (1994).
30. V. S. Ilchenko, A. A. Savchenkov, A. B. Matsko, and L. Maleki, "Nonlinear optics and crystalline whispering gallery mode cavities," Phys. Rev. Lett. **92**, 043903 (2004).
31. P. Bayvel and I. P. Giles, "Frequency generation by four wave mixing in all-fibre single-mode ring resonator," Electron. Lett. **25**, 1178–1180 (1989).
32. J. G. Provost and R. Frey, "Cavity enhanced highly nondegenerate four-wave mixing in GaAlAs semiconductor lasers," Appl. Phys. Lett. **55**, 519–521 (1989).
33. S. Murata, A. Tomita, J. Shimizu, M. Kitamura, and A. Suzuki, "Observation of highly nondegenerate four-wave mixing (>1 THz) in an InGaAsP multiple quantum well laser," Appl. Phys. Lett. **58**, 1458–1460 (1991).
34. S. Jiang and M. Dagenais, "Observation of nearly degenerate and cavity enhanced highly nondegenerate four wave mixing in semiconductor lasers," Appl. Phys. Lett. **62**, 2757–2759 (1993).
35. J. A. Hudgings and Y. Lau, "Step-tunable all-optical wavelength conversion using cavity enhanced four-wave mixing," IEEE J. Quantum Electron. **34**, 1349–1355 (1998).
36. P. P. Absil, J. H. Hryniewicz, B. E. Little, P. S. Cho, R. A. Wilson, L. G. Joneckis, and P.-T. Ho, "Wavelength conversion in GaAs micro-ring resonators," Opt. Lett. **25**, 554–556 (2000).
37. T. J. Kippenberg, S. M. Spillane, and K. J. Vahala, "Kerr-nonlinearity optical parametric oscillation in an ultra high-Q toroid microcavity," Phys. Rev. Lett. **93**, 083904 (2004).
38. A. A. Savchenkov, A. B. Matsko, D. Strekalov, M. Mohageg, V. S. Ilchenko, and L. Maleki, "Low threshold optical oscillations in a whispering gallery mode CaF_2 resonator," Phys. Rev. Lett. **93**, 243905 (2004).
39. M. Fujii, C. Koos, C. Poulton, J. Leuthold, and W. Freude, "Nonlinear FDTD analysis and experimental verification of four-wave mixing in InGaAsP–InP racetrack microresonators," IEEE Photon. Technol. Lett. **18**, 361–363 (2006).
40. A. Melloni, F. Morichetti, and M. Martinelli, "Four-wave mixing and wavelength conversion in coupled resonator optical waveguides," J. Opt. Soc. Am. B **25**, C87–C97 (2008).
41. A. C. Turner, M. A. Foster, A. L. Gaeta, and M. Lipson, "Ultra-low power parametric frequency conversion in a silicon microring resonator," Opt. Express **16**, 4881–4887 (2008).
42. M. Ferrera, L. Razzari, D. Duchesne, R. Morandotti, Z. Yang, M. Liscidini, J. E. Sipe, S. Chu, B. E. Little, and D. J. Moss, "Low-power continuous-wave nonlinear optics in doped silica glass integrated waveguide structures," Nat. Photonics **2**, 737–740 (2008).
43. L. Razzari, D. Duchesne, M. Ferrera, R. Morandotti, S. Chu, B. E. Little, and D. J. Moss, "CMOS-compatible integrated optical hyper-parametric oscillator," Nat. Photonics **4**, 41–45 (2010).
44. J. U. Furst, D. V. Strekalov, D. Elser, A. Aiello, U. L. Andersen, Ch. Marquardt, and G. Leuchs, "Low-threshold optical parametric oscillations in a whispering gallery mode resonator," Phys. Rev. Lett. **105**, 263904 (2010).
45. T. Beckmann, H. Linnenbank, H. Steigerwald, B. Sturman, D. Haertle, K. Buse, and I. Breunig, "Highly tunable low-threshold optical parametric oscillation in radially poled whispering gallery resonators," Phys. Rev. Lett. **106**, 143903 (2011).
46. C. S. Werner, T. Beckmann, K. Buse, and I. Breunig, "Blue-pumped whispering gallery optical parametric oscillator," Opt. Lett. **37**, 4224–4226 (2012).
47. G. Lin and N. Yu, "Continuous tuning of double resonance-enhanced second harmonic generation in a dispersive dielectric resonator," Opt. Express **22**, 557–562 (2014).
48. A. Chiasera, Y. Dumeige, P. Feron, M. Ferrari, Y. Jestin, G. Nunzi Conti, S. Pelli, S. Soria, and G. C. Righini, "Spherical whispering-gallery-mode microresonators," Laser Photon. Rev. **4**, 457–482 (2010).
49. G. Kozyreff, J. L. Dominguez-Juarez, and J. Martorell, "Nonlinear optics in spheres: from second harmonic scattering to quasi-phase matched generation in whispering gallery modes," Laser Photon. Rev. **5**, 737–749 (2011).
50. A. A. Savchenkov, V. S. Ilchenko, A. B. Matsko, and L. Maleki, "Kilohertz optical resonances in dielectric crystal cavities," Phys. Rev. A **70**, 051804(R) (2004).
51. A. A. Savchenkov, A. B. Matsko, V. S. Ilchenko, and L. Maleki, "Optical resonators with ten million finesse," Opt. Express **15**, 6768–6773 (2007).
52. T. J. Kippenberg and K. J. Vahala, "Cavity optomechanics: back-action at the mesoscale," Science **321**, 1172–1176 (2008).
53. I. S. Grudinin and L. Maleki, "Ultralow-threshold Raman lasing with CaF_2 resonators," Opt. Lett. **32**, 166–168 (2007).
54. P. Del-Haye, T. Herr, E. Gavartin, M. L. Gorodetsky, R. Holzwarth, and T. J. Kippenberg, "Octave spanning tunable frequency comb from a microresonator," Phys. Rev. Lett. **107**, 063901 (2011).
55. Y. Okawachi, K. Saha, J. S. Levy, Y. H. Wen, M. Lipson, and A. L. Gaeta, "Octave spanning frequency comb generation in a silicon nitride chip," Opt. Lett. **36**, 3398–3400 (2011).
56. I. S. Grudinin, A. B. Matsko, A. A. Savchenkov, D. Strekalov, V. S. Ilchenko, and L. Maleki, "Ultra-high *Q* crystalline microcavities," Opt. Commun. **265**, 33–38 (2006).

57. H. Tavernier, N. N. T. Kim, P. Feron, R. Bendoula, P. Salzenstein, E. Rubiola, and L. Larger, "Optical disk resonators with micro-wave free spectral range for optoelectronic oscillator," in *Proceedings of the 22nd European Time and Frequency Forum*, Toulouse, France, 2008, paper FPE-0179.
58. H. Tavernier, P. Salzenstein, K. Volyanskiy, Y. K. Chembo, and L. Larger, "Magnesium fluoride whispering gallery mode disk-resonators for microwave photonics applications," IEEE Photon. Technol. Lett. **22**, 1629–1631 (2010).
59. W. Liang, A. A. Savchenkov, A. B. Matsko, V. S. Ilchenko, D. Seidel, and L. Maleki, "Generation of near-infrared frequency combs from a MgF_2 whispering gallery mode resonator," Opt. Lett. **36**, 2290–2292 (2011).
60. I. S. Grudinin, L. Baumgartel, and N. Yu, "Frequency comb from a microresonator with engineered spectrum," Opt. Express **20**, 6604–6609 (2012).
61. A. B. Matsko, A. A. Savchenkov, D. Strekalov, V. S. Ilchenko, and L. Maleki, "Optical hyperparametric oscillations in a whispering-gallery-mode resonator: threshold and phase diffusion," Phys. Rev. A **71**, 033804 (2005).
62. M. Haelterman, S. Trillo, and S. Wabnitz, "Additive-modulation-instability ring laser in the normal dispersion regime of a fiber," Opt. Lett. **17**, 745–747 (1992).
63. S. Coen and M. Haelterman, "Modulational instability induced by cavity boundary conditions in a normally dispersive optical fiber," Phys. Rev. Lett. **79**, 4139–4142 (1997).
64. Y. K. Chembo and N. Yu, "Modal expansion approach to optical-frequency-comb generation with monolithic whispering-gallery-mode resonators," Phys. Rev. A **82**, 033801 (2010).
65. A. Matsko, A. Savchenkov, W. Liang, V. Ilchenko, D. Seidel, and L. Maleki, "Group velocity dispersion and stability of resonant hyper-parametric oscillations," in *Nonlinear Optics: Materials, Fundamentals and Applications*, OSA Technical Digest (CD) (Optical Society of America, 2011), paper NWD2.
66. A. B. Matsko, A. A. Savchenkov, and L. Maleki, "Normal group-velocity dispersion Kerr frequency comb," Opt. Lett. **37**, 43–45 (2012).
67. C. Godey, I. V. Balakireva, A. Coillet, and Y. K. Chembo, "Stability analysis of the spatiotemporal Lugiato–Lefever model for Kerr optical frequency combs in the anomalous and normal dispersion regimes," Phys. Rev. A **89**, 063814 (2014).
68. T. Hansson, D. Modotto, and S. Wabnitz, "Dynamics of the modulational instability in microresonator frequency combs," Phys. Rev. A **88**, 023819 (2013).
69. A. Coillet, I. Balakireva, R. Henriet, K. Saleh, L. Larger, J. M. Dudley, C. R. Menyuk, and Y. K. Chembo, "Azimuthal Turing patterns, bright and dark cavity solitons in Kerr combs generated with whispering-gallery-mode resonators," IEEE Photon. J. **5**, 6100409 (2013).
70. W. Liang, A. A. Savchenkov, V. S. Ilchenko, D. Eliyahu, D. Seidel, A. B. Matsko, and L. Maleki, "Generation of a coherent near-infrared Kerr frequency comb in a monolithic microresonator with normal GVD," Opt. Lett. **39**, 2920–2923 (2014).
71. A. A. Savchenkov, A. B. Matsko, W. Liang, V. S. Ilchenko, D. Seidel, and L. Maleki, "Kerr frequency comb generation in overmoded resonators," Opt. Express **20**, 27290–27298 (2012).
72. Y. Liu, Y. Xuan, X. Xue, P.-H. Wang, S. Chen, A. J. Metcalf, J. Wang, D. E. Leaird, M. Qi, and A. M. Weiner, "Investigation of mode coupling in normal-dispersion silicon nitride microresonators for Kerr frequency comb generation," Optica **1**, 137–144 (2014).
73. T. Herr, V. Brasch, J. D. Jost, I. Mirgorodskiy, G. Lihachev, M. L. Gorodetsky, and T. J. Kippenberg, "Mode spectrum and temporal soliton formation in optical microresonators," Phys. Rev. Lett. **113**, 123901 (2014).
74. S. Ramelow, A. Farsi, S. Clemmen, J. S. Levy, A. R. Johnson, Y. Okawachi, M. R. E. Lamont, M. Lipson, and A. L. Gaeta, "Strong polarization mode coupling in microresonators," Opt. Lett. **39**, 5134–5137 (2014).
75. W. Liang, A. Savchenkov, J. McMillan, Z. Xie, V. Ilchenko, D. Seidel, C. W. Wong, A. B. Matsko, and L. Maleki, "Strongly nondegenerate resonant optical parametric oscillator," in *Nonlinear Optics*, B. Boulanger, S. Cundiff, M. Kauranen, and W. Knox, eds., OSA Technical Digest (online) (Optical Society of America, 2013), paper NF1A.5.
76. T. Carmon and K. J. Vahala, "Visible continuous emission from a silica microphotonic device by third-harmonic generation," Nat. Phys. **3**, 430–435 (2007).
77. J. S. Levy, M. A. Foster, A. L. Gaeta, and M. Lipson, "Harmonic generation in silicon nitride ring resonators," Opt. Express **19**, 11415–11421 (2011).
78. D. Farnesi, A. Barucci, G.-C. Righini, S. Berneschi, S. Soria, and G. Nunzi Conti, "Optical frequency conversion in silica-whispering-gallery-mode microspherical resonators," Phys. Rev. Lett. **112**, 093901 (2014).
79. I. S. Grudinin and N. Yu, "Micro-structured crystalline resonators for optical frequency comb generation," arXiv:1406.2682, 2014.
80. B. Dahmani, L. Hollberg, and R. Drullinger, "Frequency stabilization of semiconductor lasers by resonant optical feedback," Opt. Lett. **12**, 876–878 (1987).
81. L. Hollberg and M. Ohtsu, "Modulatable narrow-linewidth semiconductor lasers," Appl. Phys. Lett. **53**, 944–946 (1988).
82. A. Hemmerich, C. Zimmermann, and T. W. Hänsch, "Compact source of coherent blue light," Appl. Opt. **33**, 988–991 (1994).
83. W. Liang, V. S. Ilchenko, A. A. Savchenkov, A. B. Matsko, D. Seidel, and L. Maleki, "Whispering-gallery-mode-resonator-based ultra-narrow linewidth external-cavity semiconductor laser," Opt. Lett. **35**, 2822–2824 (2010).
84. M. R. E. Lamont, Y. Okawachi, and A. L. Gaeta, "Route to stabilized ultrabroadband microresonator-based frequency combs," Opt. Lett. **38**, 3478–3481 (2013).
85. T. Herr, V. Brasch, J. D. Jost, C. Y. Wang, N. M. Kondratiev, M. L. Gorodetsky, and T. J. Kippenberg, "Temporal solitons in optical microresonators," Nat. Photonics **8**, 145–152 (2014).
86. C. C. Lam, P. T. Leung, and K. Young, "Explicit asymptotic formulas for the positions, widths, and strengths of resonances in Mie scattering," J. Opt. Soc. Am. B **9**, 1585–1592 (1992).
87. M. L. Gorodetsky and A. E. Fomin, "Geometrical theory of whispering gallery modes," IEEE J. Sel. Top. Quantum Electron. **12**, 33–39 (2006).
88. M. Sumetsky, "Whispering-gallery-bottle microcavities: the three-dimensional etalon," Opt. Lett. **29**, 8–10 (2004).
89. A. A. Savchenkov, A. B. Matsko, W. Liang, V. S. Ilchenko, D. Seidel, and L. Maleki, "Kerr combs with selectable central frequency," Nat. Photonics **5**, 293–296 (2011).